

PII:S0026-2692(96)00118-8

The physics and fabrication of *in situ* back-gated (311)A hole gas heterojunctions

M.Y. Simmons, A.R. Hamilton, A. Kurobe,
S.J. Stevens, D.A. Ritchie and M. Pepper

Cavendish Laboratory, Madingley Road, Cambridge CB3 0HE, UK

This paper reports the fabrication of an *in situ* back-gated hole gas on the (311)A surface of GaAs. The hole density can be varied from fully depleted to $p_s = 2.1 \times 10^{11} \text{ cm}^{-2}$ with mobilities of up to $\mu = 1.1 \times 10^6 \text{ cm}^2 \text{ V}^{-1} \text{ s}^{-1}$. It is seen that for carrier densities down to $p_s = 4 \times 10^{10} \text{ cm}^{-2}$ the mobility in the $[\bar{2}33]$ direction is greater than that in the $[01\bar{1}]$ direction. Using a combination of front- and back-gates we are able to keep the carrier density constant and deform the hole gas wavefunction such that the holes are pushed up against or moved further away from the heterointerface. Thus we are able to separately investigate the various scattering mechanisms that determine the mobility, and compare the experimental data with theoretical calculations based on the shape of the wavefunction. © 1997 Elsevier Science Ltd.

There has been considerable recent interest in the transport properties of two dimensional hole gases (2DHGs) in GaAs/AlGaAs heterostructures fabricated by molecular beam epitaxy (MBE). In order to obtain the high mobility necessary to see quantum behaviour [1, 2], samples have been fabricated on the (311)A surface of GaAs, where silicon is incorporated as an acceptor, rather than the usual

(100) surface where beryllium is typically used as the acceptor. One of the properties of using this surface is that the mobility is found to be strongly anisotropic; the mobility in the $[\bar{2}33]$ direction being greater than that in the $[01\bar{1}]$ direction [2, 3]. This mobility anisotropy was initially thought to arise from the anisotropy in the Fermi surface leading to different effective masses in the $[\bar{2}33]$ and $[01\bar{1}]$ directions [2]. However, the magnitude of the measured mobility ratios was observed to be too substantial to be fully explained by this effect and has more recently been ascribed to anisotropic interface roughness scattering [3]. Using a front-gated hole gas fabricated on the (311)A surface of GaAs, Heremans *et al.* were able to observe the effect of changing the carrier density on the mobility in the two orthogonal directions.

In this paper we describe the use of a back-gate below the 2DHG, such that using a combination of front- and back-gates we are able to have independent control over both the shape of the

hole wavefunction and the carrier density. In particular, whilst keeping the carrier density constant we are able to deform the hole gas wavefunction, moving the holes either close to or away from the heterointerface. This allows us to separate those scattering mechanisms which only depend on the carrier density, from those that are also sensitive to the shape of the wavefunction. Using a simple model to predict the mobility anisotropy as a function of carrier density, reasonable agreement was obtained with experiment at high carrier densities ($p_s > 1.0 \times 10^{11} \text{ cm}^{-2}$) but the model could not fully account for the persistence of the anisotropy observed at low carrier densities.

The samples used in this study were grown *simultaneously* on (a) n^+ doped and (b) undoped (311)A GaAs substrates mounted side by side on a molybdenum block. The MBE growth consisted of 200 Å GaAs, a 2000 Å $\text{Al}_{0.33}\text{Ga}_{0.67}\text{As}$ back-barrier layer, 2 μm GaAs, 500 Å undoped $\text{Al}_{0.33}\text{Ga}_{0.67}\text{As}$ spacer layer, 2000 Å $\text{Al}_{0.33}\text{Ga}_{0.67}\text{As}$ doped at $1.0 \times 10^{17} \text{ cm}^{-3}$ and a 170 Å GaAs capping layer. The advantages of using a conducting substrate are that the 2DHG is situated only 2 μm from the back-gate and is certain to be parallel to the 2DHG. Thus, only

small back-gate biases are required to control the carrier density, and the back-gate does not produce any inhomogeneities in the hole gas, even at low densities. The wafer was processed into an orthogonal Hall bar geometry with AuBe ohmic contacts to the 2DHG, and a NiCr/Au front Schottky gate. AuGeNi was evaporated onto the rear side of the wafer to form an ohmic contact to the back-gate. Magnetotransport measurements were carried out at 1.7 K and 30 mK. The back-gate could be operated in the range $-0.5 \text{ V} < V_{\text{bg}} < 1.1 \text{ V}$, and the front-gate in the range $-0.4 \text{ V} < V_{\text{fg}} < 0.1 \text{ V}$, with gate leakage currents below 2 nA. The carrier density p_s was found to vary linearly both with front- and back-gate bias, such that $\partial p_s / \partial V_g$ agreed to within 8% of the values expected from a simple capacitor model using the distances between the 2DHG and gates obtained from the growth specifications.

Figure 1 shows the magnetoresistance (R_{xx}) and Hall resistance (R_{xy}) for both the [011] and $[\bar{2}33]$ directions as a function of magnetic field, with $V_{\text{fg}} = V_{\text{bg}} = 0 \text{ V}$ and $T = 30 \text{ mK}$. Clear integer and fractional quantum Hall states are observed up to 11 T; below $\nu = 1/3$ an insulating phase occurs as observed in ungated hole gas samples of similar quality [4, 5]. The inset shows the

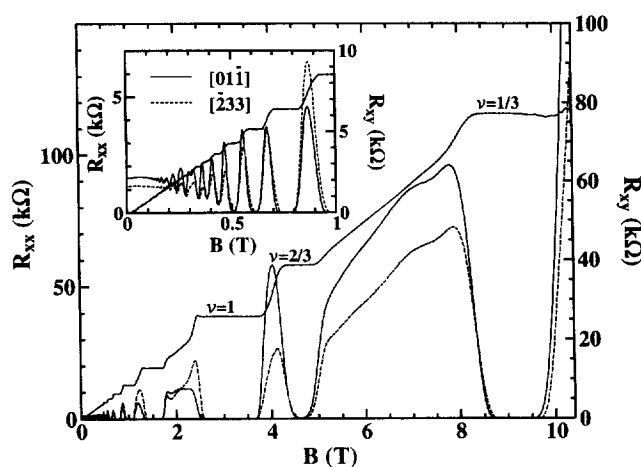


Fig. 1. Magnetoresistance (R_{xx}) and Hall resistance (R_{xy}) for both the [011] and $[\bar{2}33]$ directions with $V_{\text{bg}} = V_{\text{fg}} = 0$ at 30 mK. The inset shows the low-field data, highlighting the anisotropy in the zero field resistance.

low-field data, where the mobility anisotropy between the $[233]$ and $[01\bar{1}]$ directions can clearly be seen. At this carrier density ($p_s=0.71\times 10^{11}\text{ cm}^{-2}$) the mobility ratio between the two directions is observed to be approximately 1.34, compared with a ratio of 1.67 at the highest carrier density measured. Using a combination of both front- and back-gates we were able to change the carrier density in these samples from fully depleted to $p_s=2.1\times 10^{11}\text{ cm}^{-2}$ with mobilities of up to $=1.1\times 10^6\text{ cm}^2\text{ V}^{-1}\text{ s}^{-1}$.

By comparing the carrier densities obtained from Hall bars (without front-gates) fabricated on undoped and n^+ substrates, we are able to determine the nature of the interface states on undoped (311)A substrates. The sample grown on the semi-insulating substrate had a carrier density of $p_s=2.1\times 10^{11}\text{ cm}^{-2}$, compared to a carrier density of $p_s=7.8\times 10^{10}\text{ cm}^{-2}$ for the sample grown on the n^+ substrate at $V_{\text{bg}}=0\text{ V}$. The difference in carrier densities on these two different samples gives a direct measure of the difference in pinning of the Fermi energy at the substrate interface. From measurements of $\partial p_s/\partial V_{\text{bg}}$ we find that this difference in carrier densities ($0.42\times 10^{11}\text{ cm}^{-2}$) implies a difference in the pinning of 1.4V. Given that the Fermi energy in the n^+ substrate must lie in the conduction band, the Fermi energy in the undoped (311)A substrate appears to be close to the valence band at the interface. This implies that either (a) there is a residual background p-type doping in the nominally undoped substrate, or (b) that there are very few interface states at the growth interface, or (c) that the states are close in energy to the valence band edge. The use of a doped substrate as the back-gate, however, is seen to have no adverse effect on the sample quality; the sample grown on the semi-insulating substrate had a mobility of $\mu_{[233]}=6.2\times 10^5\text{ cm}^2\text{ V}^{-1}\text{ s}^{-1}$ at $T=1.7\text{ K}$, compared to $\mu_{[233]}=6.8\times 10^5\text{ cm}^2\text{ V}^{-1}\text{ s}^{-1}$ for the sample grown on the n^+ substrate at the

same carrier density ($p_s=1.2\times 10^{11}\text{ cm}^{-2}$, $V_{\text{fg}}=-0.15\text{ V}$, $V_{\text{bg}}=-0.1\text{ V}$).

Figure 2a shows the mobilities (measured at 30mK) in both the $[233]$ and $[01\bar{1}]$ directions as a function of carrier density, obtained by sweeping the front-gate from -0.4 V to $+0.1\text{ V}$ at incremental back-gate biases of 0.05 V . It can be seen that for all back-gate biases there exists a mobility anisotropy, which increases with increasing carrier density. At low carrier densities (below $4.0\times 10^{10}\text{ cm}^{-2}$) the anisotropy is observed to disappear. Initially, it was believed that the mobility anisotropy in hole gases was due to the anisotropic hole effective mass [2]. However, it was later observed that 2D electron gases (which have an isotropic mass) grown on the (311)B surface of GaAs were also found to exhibit a similar mobility anisotropy [6]. On closer inspection of Fig. 2a it can be seen that there is a marked difference in the carrier dependence of the mobility in the two orthogonal directions. As V_{fg} is made more negative (increasing the carrier density) the mobility along the $[233]$ direction is observed to continuously increase, in contrast to $\mu_{[01\bar{1}]}$, where above a certain carrier density the mobility starts to decrease. This decrease has been observed previously [3] and has been attributed to the increasing importance of anisotropic interface roughness scattering in the $[01\bar{1}]$ direction at high carrier densities. Scanning tunnelling microscopy (STM) studies [7] have confirmed that the (311)A surface of GaAs reconstructs to form quasi-periodic corrugations perpendicular to the $[233]$ direction, with a period of 32 \AA and height of two monolayers ($3.4\pm 0.4\text{ \AA}$). This mesoscopic roughening of the surface is thought to account for the mobility anisotropy observed in both 2DHGs and 2DEGs formed on $\{311\}$ surfaces, although it is not clear from the STM studies whether these corrugations observed would persist at a heterointerface. The STM images also revealed the presence of anisotropic island growth, with large (100 \AA

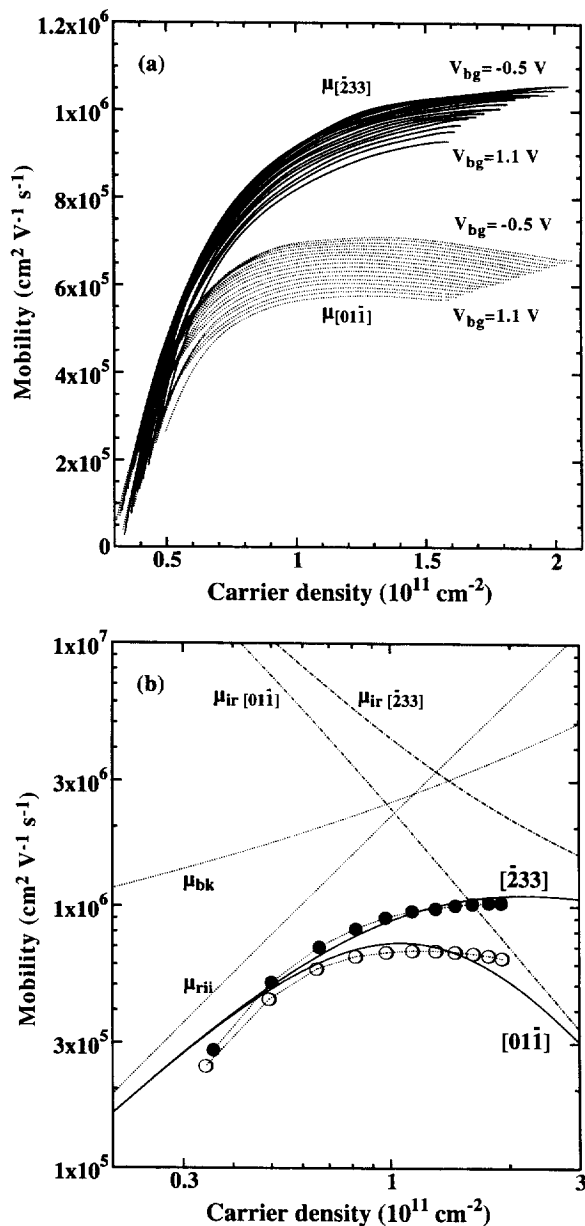


Fig. 2. (a) Experimental mobilities as a function of carrier density for both the $[01\bar{1}]$ and $[\bar{2}33]$ directions obtained by sweeping the front-gate at incremental values of 0.05 V in the back-gate voltage. (b) Experimentally measured and theoretically calculated mobilities as a function of carrier density for $V_{bg}=0$ V. The solid lines show the theoretical mobilities due to the combined scattering mechanisms in the two directions; the experimental data is marked with symbols.

diameter) islands elongated along the $[\bar{2}33]$ direction.

In order to understand the physical mechanisms determining the mobility in this sample, a simple calculation of the mobility in the two orthogonal directions, taking into account the deformation of the wavefunction by the back-gate voltage, was performed. Scattering from the following sources was considered when calculating the total mobility: (i) remote ionised impurities (μ_{rii}); (ii) anisotropic interface roughness ($\mu_{ir[\bar{2}33]}$, $\mu_{ir[01\bar{1}]}$); and (iii) residual impurity scattering (μ_{bk}). The calculations were performed for $T=0$ K, using a Fang–Howard wavefunction, with screening included in the long wavelength limit. The effect of the back-gate on the shape of the hole wavefunction was included in the calculation as described in Ref. [8] – essentially the back-gate bias determines the electric field E_{bg} in the substrate far from the heterointerface. In this approach the depletion charge is set to zero. [The depletion charge is given by $N_{depl}=(2\epsilon_L N_{bk}\phi_A/e)^{1/2}$ where N_{bk} is the background doping density and ϕ_A is the acceptor ionisation energy. Assuming the background doping is p-type, we find that for $N_{bk}<10^{14}$ cm $^{-3}$ and $\phi_A\approx 10$ meV, $N_{depl}\leq 4\times 10^9$ cm $^{-2}$. Thus $p_s\gg N_{depl}$ for the range of carrier densities studied here, justifying the approximation $N_{depl}=0$.] The variational parameter b in the Fang–Howard wavefunction $\psi(z) = b^{3/2}/(2\sqrt{2})z \exp(-bz/2)$ is given by:

$$b^3 = \frac{8m_z^*}{\hbar^2} \left(\frac{33e^2 p_s}{64\epsilon_L} - \frac{3eE_{bg}}{4} \right) \quad (1)$$

where m_z^* is the effective mass perpendicular to the heterojunction, ϵ_L is the dielectric constant of GaAs, and b^{-1} is a measure of the width of the 2D hole gas.

The mobilities μ_{rii} and μ_{bk} were calculated as described in Ref. [9], whilst calculation of the interface roughness scattering [10] was modified such that the effective field at the

heterointerface F_{eff} now includes a term due to the back-gate:

$$F_{\text{eff}} = \int dz |\psi(z)|^2 \frac{\delta U}{\delta z} = \frac{p_s e^2}{2\epsilon_L} + eE_{\text{bg}} \quad (2)$$

where $U(z)$ is the potential energy. In this equation the front-gate bias is represented by the dependence of F_{eff} on p_s and so does not appear explicitly. The interface roughness is defined by three parameters: the amplitude of the roughness Δ , and two (Gaussian) correlation lengths $\Lambda_{[233]}$ and $\Lambda_{[01\bar{1}]}$. The anisotropy of the scattering rate was incorporated using a method described in Ref. [11].

It is worth mentioning that in these samples only the heavy hole band is occupied (the light hole band being ≈ 10 meV from the Fermi energy). The asymmetric confining potential in a single heterojunction leads to a lifting of the spin degeneracy away from $\mathbf{k}=0$ at $B=0$ [12]. To account for this we have used a two band model, with effective masses of $0.23m_e$ and $0.38m_e$ for the two hole species [3], but have neglected the possibility of intersubband scattering. Finally the mobilities due to the various scattering mechanisms were combined using Matthiessen's rule, to obtain the total mobilities $\mu_{[233]}$ and $\mu_{[01\bar{1}]}$.

Figure 2b shows both the experimental (lines with symbols) and theoretical values of $\mu_{[233]}$ and $\mu_{[01\bar{1}]}$ as a function of carrier density, for a back-gate bias of $V_{\text{bg}}=0$ V. The dashed lines in the figure illustrate the calculated mobilities for the various scattering mechanisms, using fitting parameters of $N_{\text{doping}}=0.6 \times 10^{17} \text{ cm}^{-3}$, $N_{\text{bk}}=5 \times 10^{13} \text{ cm}^{-3}$, $\Delta=2 \text{ \AA}$, $\Lambda_{[233]}=130 \text{ \AA}$ and $\Lambda_{[01\bar{1}]}=32 \text{ \AA}$. The parameters used in the calculations agree well with the experimental growth conditions used, and the expected size and height of the mesoscopic surface roughness mentioned earlier. The same parameters were found to give good agreement between theory and experiment for all back-gate biases studied. From the model we can see that at high p_s the

mobility is limited by the interface roughness scattering and is thus highly anisotropic. As the carrier density is reduced the dominant scattering mechanism changes from interface roughness scattering to remote ionised impurity scattering, and the mobility thus decreases and becomes more isotropic. The experimental data is in good agreement with the calculated mobilities, although we find that at low p_s the mobility anisotropy does not disappear as fast as the calculations suggest. Better agreement with the experimental data at lower carrier densities can be achieved by altering the correlation lengths $\Lambda_{[233]}$ and $\Lambda_{[01\bar{1}]}$. By using larger island sizes in the calculations, it was possible to reproduce the mobility anisotropy observed at low carrier densities, but significantly worse agreement was then found at higher carrier densities. These results are consistent with the STM studies of the (311)A surface. At high carrier densities the mobility is dominated by scattering from the quasi-periodic (32 Å) corrugations and is thus highly anisotropic. At lower carrier densities it is the large irregular islands that are important in determining the interface roughness scattering.

Using a combination of front- and back-gate biases we are able to keep the carrier density constant, whilst deforming the envelope wavefunction such that the holes are moved towards or away from the heterointerface. Figure 3a shows the mobility ratio $\mu_{[233]}/\mu_{[01\bar{1}]}$, measured at several different carrier densities as a function of back-gate bias. It can be seen that at all carrier densities from $p_s=2.0 \times 10^{11} \text{ cm}^{-2}$ down to $p_s=0.5 \times 10^{11} \text{ cm}^{-2}$, the effect of increasing the back-gate bias is to increase the mobility ratio. By increasing the back-gate bias we are effectively pushing the hole wavefunction up against the heterointerface, leading to a reduction in the mobility in both the [233] and [01 $\bar{1}$] directions. Since interface roughness scattering is more important in determining the mobility in the [01 $\bar{1}$] direction than in the [233] direction, $\mu_{[01\bar{1}]}$ will decrease more rapidly with V_{bg} than $\mu_{[233]}$, hence the increase in the mobility ratio. Figure 3b shows a theoretical fit to

the experimental data of the mobilities in the $\mu_{[233]}$ and $\mu_{[01\bar{1}]}$ directions for $p_s=1.25 \times 10^{11} \text{ cm}^{-2}$ as a function of V_{bg} . The same fitting parameters are used as in Fig. 2b. It can be seen that both the background and remote ionised impurity scattering rates are almost independent of the back-gate bias, as they are primarily determined by the Fermi wavevector k_F (and hence by the carrier density). The anisotropic interface roughness scattering however is sensitive to the shape of the wavefunction, so increasing V_{bg} causes the mobilities in both the $[233]$ and $[01\bar{1}]$ directions to decrease, although not at the same rate. The fit is shown here for one carrier density, but was found to be in good agreement for all carrier densities presented in Fig. 3a. The inset to Fig. 3b shows a good fit to the mobility ratio obtained from modelling the data at one fixed carrier density, confirming the validity of the simple model.

The data presented so far has been for carrier densities down to $p_s=3.0 \times 10^{10} \text{ cm}^{-2}$, at which point the mobilities in the orthogonal directions

become equal. However, the ability to vary the mobility at a fixed carrier density (e.g. at $p_s=4.0 \times 10^{10} \text{ cm}^{-2}$ the μ can be varied by a factor of two) is in itself useful, for example in the study of the effect of disorder upon the quantum Hall effect and metal-insulator transitions. In Fig. 4 we show the beginning of such studies, plotting the diagonal resistivity ρ_{xx} as a function of B in the very low carrier density regime. The front-gate bias is held constant at 0.1 V, and traces are shown for $0 \text{ V} < V_{bg} < 0.4 \text{ V}$. Further increase of the back-gate bias depletes the hole gas completely. The insulating phase occurring above $\nu=1/3$ at higher carrier densities moves to higher filling factors as p_s has been reduced, reaching $\nu=1$ at a carrier density of $p_s=3.0 \times 10^{10} \text{ cm}^{-2}$. At the lowest carrier densities the mobility drops very suddenly (inset to Fig. 4), which has been taken as evidence of a metal-insulator transition due to multiple scattering events [9].

In summary we have reported the fabrication of the first *in situ* high mobility back-gated GaAs-

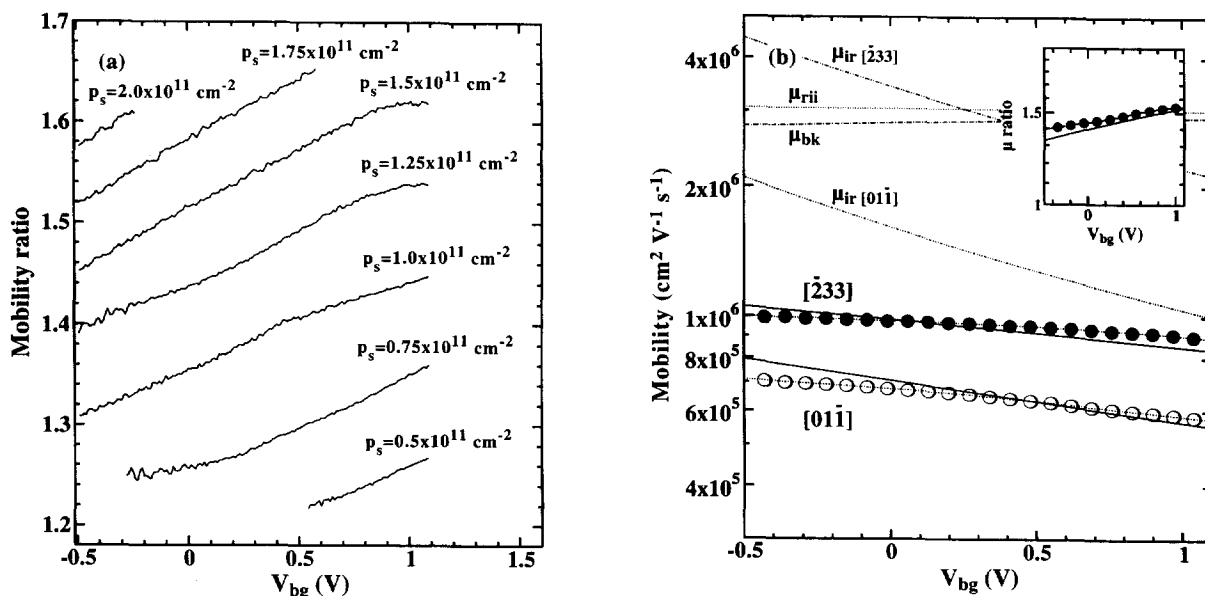


Fig. 3. (a) The measured mobility ratio $\mu_{[233]}/\mu_{[01\bar{1}]}$ as a function of V_{bg} for different carrier densities. (b) Experimentally measured and theoretically calculated mobilities as a function of V_{bg} for $p_s=1.25 \times 10^{11} \text{ cm}^{-2}$. The inset shows the measured (symbols) and calculated (solid line) mobility ratio.

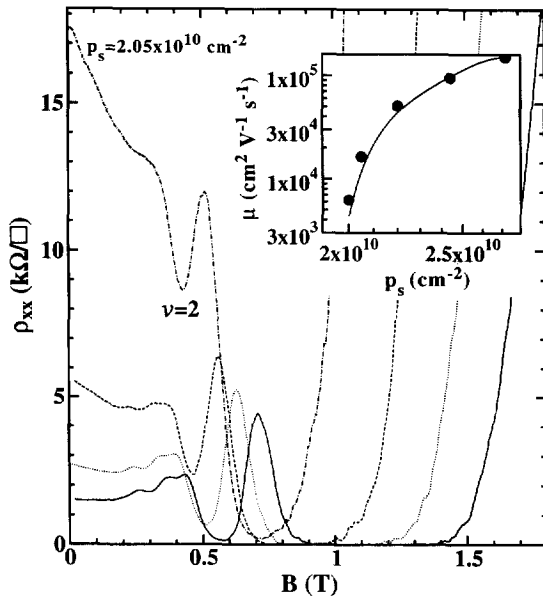


Fig. 4. The magnetoresistivity ρ_{xx} along the $[233]$ direction measured at 30 mK. The lowest trace is for $p_s = 2.7 \times 10^{10} \text{ cm}^{-2}$, subsequent traces are for 2.4, 2.2 and $2.0 \times 10^{10} \text{ cm}^{-2}$ as V_{bg} is increased in steps of 0.1 V. The inset shows the dramatic reduction in the mobility as p_s is reduced.

AlGaAs 2D hole gas. The scattering mechanisms limiting the mobility have been investigated both theoretically and experimentally and related to recent STM studies of the (311)A GaAs surface. In particular, we have demonstrated how a combination of back- and front-gates can be used to deform the hole gas wavefunction and therefore alter the relative importance of interface roughness and ionised impurity scattering at constant carrier density.

Acknowledgment

This work was funded by EPSRC (UK).

References

- [1] Zailer, I., Frost, J.E.F., Ford, C.J.B., Pepper, M., Simmons, M.Y., Ritchie, D.A., Nicholls, J.T. and Jones, G.A.C. Phase coherence, interference, and conductance quantisation in a confined 2DHG. *Phys. Rev. B*, 49 (1994) 5101.
- [2] Davies, A.G., Frost, J.E.F., Ritchie, D.A., Peacock, D.C., Newbury, R., Linfield, E.H., Pepper, M. and Jones, G.A.C. The growth and physics of high mobility 2D hole gases. *J. Crystal Growth*, 111 (1991) 318.
- [3] Heremans, J.J., Santos, M.B., Hirakawa, K. and Shayegan, M. Mobility anisotropy of two dimensional hole systems in (311)A GaAs/AlGaAs heterojunctions. *J. Appl. Phys.*, 76 (1994) 1980.
- [4] Santos, M.B., W Sven, Y., Shayegan, M., Li, Y.P., Engel, L.W. and Tsui, D.C. Observation of re-entrant insulating phase near $1/3$ fractional quantum Hall liquids in 2D hole systems. *Phys. Rev. Lett.*, 68 (1992) 1188.
- [5] Manoharan, H.C. and Shayegan, M. Wigner crystal versus Hall insulator. *Phys. Rev. B*, 50 (1994) 17662.
- [6] Churchill, A.C., Kim, G.H., Kurobe, A., Simmons, M.Y., Ritchie, D.A., Pepper, M. and Jones, G.A.C. Anisotropic magnetotransport in 2DEGs on (311)B GaAs substrates. *J. Phys. Condens. Matter*, 6 (1994) 6131.
- [7] Wassermeier, M., Sudijono, J., Johnson, M.D., Leung, K.T., Orr, B.G., Daweritz L. and Ploog, K. Reconstruction of GaAs (311)A surface. *Phys. Rev. B*, 51 (1995) 14721; STM of GaAs (311)A surface reconstruction, *J. Crystal Growth*, 150 (1995) 425.
- [8] Kelly, M.J. and Hamilton, A. The electronic structure of a back-gated high electron mobility transistor. *Semicond. Sci. Technol.*, 6 (1991) 201.
- [9] Gold, A. Mobility of the two-dimensional electron gas in AlGaAs/GaAs heterostructures at low electron densities. *Appl. Phys. Lett.*, 54 (1989) 2100.
- [10] Ando, T. Self-consistent results for a GaAs/AlGaAs heterojunction II. Low temperature mobility. *J. Phys. Soc. Jpn.*, 51 (1982) 3900.
- [11] Nag, B.R. *Electron Transport in Compound Semiconductor Structures, Springer Series in Solid State Sciences II*, Springer, Berlin, 1980.
- [12] Eisenstein, J.P., Stormer, H.L., Narayanamurti, V., Gossard, A.C. and Wiegmann, W. Effect of inversion symmetry on the band structure of semiconductor heterostructures. *Phys. Rev. Lett.*, 53 (1984) 25793.